Received: 9 December 2018 | Accepted: 21 January 2019

DOI: 10.1002/ame2.12059

ORIGINAL ARTICLE

Knockout of *ISCA1* causes early embryonic death in rats

Xinlan Yang[1] | Dan Lu[2] | Xu Zhang[2] | Wei Chen[1] | Shan Gao[1] | Wei Dong[1] | Yuanwu Ma[2,3] | Lianfeng Zhang[1,3]

[1]Key Laboratory of Human Disease Comparative Medicine, National Health Commission of China (NHC), Institute of Laboratory Animal Science, Peking Union Medical College, Chinese Academy of Medical Sciences, Beijing, China

[2]Beijing Engineering Research Center for Experimental Animal Models of Human Diseases, Institute of Laboratory Animal Science, Peking Union Medical College, Chinese Academy of Medical Sciences, Beijing, China

[3]Neuroscience Center, Chinese Academy of Medical Sciences, Beijing, China

Correspondence
Lianfeng Zhang, Key Laboratory of Human Disease Comparative Medicine, National Health Commission of China (NHC), Institute of Laboratory Animal Science, Peking Union Medical College, Chinese Academy of Medical Sciences, Beijing, China.
Email: zhanglf@cnilas.org

Funding information
CAMS Innovation Fund for Medical Sciences, Grant/Award Number: 2017-I2M-3-015 and 2016-I2M-1-004

Abstract

Background: Iron-sulfur cluster assembly 1 (ISCA1) is an iron-sulfur (Fe/S) carrier protein that accepts Fe/S from a scaffold protein and transfers it to target proteins including the mitochondrial Fe/S containing proteins. *ISCA1* is also the newly identified causal gene for multiple mitochondrial dysfunctions syndrome (MMDS). However, our knowledge about the physiological function of ISCA1 in vivo is currently limited. In this study, we generated an *ISCA1* knockout rat line and analyzed the embryo development.

Methods: *ISCA1* knockout rats were generated by replacing the exon1 of *ISCA1* gene with the *mCherry-Cre* fusion gene using CRISPR-Cas9 technology. The ISCA1 expression pattern was analyzed by fluorescence imaging using ISCA1 promotor driven Cre and mCherry expression. The embryonic morphology was examined by microscope and mitochondrial proteins were tested by Western blot.

Results: An *ISCA1* knockout rat line was obtained, which expressed mCherry-Cre fusion protein. Both of the fluorescence images from mCherry and Cre induced mCherry in a reporter rat strain, showing that ISCA1 expressed in most of the tissues in rats. The ISCA1 knockout resulted in abnormal development at 8.5 days, with a significant decrease of NDUFA9 protein and an increase of aconitase 2 (ACO2) in rat embryos.

Conclusion: Deletion of *ISCA1* induced early death in rats. ISCA1 affected the expression of key proteins in the mitochondrial respiratory chain complex, suggesting that ISCA1 has an important influence on the respiratory complex and energy metabolism.

KEYWORDS
embryonic development, energy metabolism, ISCA1

1 | INTRODUCTION

Iron-sulfur clusters (Fe/S) are essential cofactors for a number of cellular processes including mitochondrial respiration and DNA metabolism.[1,2] The homologues of Fe/S clusters are highly conserved and present in bacteria, yeast, and mammalia.[3-6] In bacteria there are at least three distinct types of Fe/S cluster assembly machinery, which are involved in cysteine desulfurase-mediated

assembly of transient clusters on scaffold proteins, and are known as the nitrogen fixation (NIF), iron-sulfur cluster (ISC) and sulfur assimilation (SUF) systems.[7] In mammalia, including mice and humans, Fe/S protein biogenesis is initiated in the mitochondria, where the persulfide is reduced to sulfide with the help of a ferredoxin electron transport system comprising ferredoxin reductase and ferredoxin 2.[8,9] Sulfide then forms a [2Fe-2S] cluster with ferrous iron (Fe^{2+}) on scaffold proteins such as iron-sulfur cluster assembly enzyme (ISCU), which supports the assembly of a subset of Fe/S apoproteins.[10]

The homologues of bacterial ISC in mammalia are iron-sulfur cluster assembly 1 (ISCA1) and iron-sulfur cluster assembly 2 (ISCA2), which are related to Isa1 and Isa2, respectively, in eukaryocytes.[10,11] ISCA1 and ISCA2 behave as Fe/S carriers, accepting Fe/S from a scaffold protein and transferring it to target proteins, and function as important Fe/S cluster assembly machinery in mammalian cells. In HeLa cells, knockdown of *ISCA1* and *ISCA2* resulted in a decrease of the activities of mitochondrial Fe/S proteins, including aconitase, respiratory complex I, and lipoic acid synthase, through the ISC assembly pathway.[10,12] *ISCA1* and *ISCA2* are the causal genes for multiple mitochondrial dysfunctions syndrome (MMDS). Mutations of *ISCA1* and *ISCA2* cause severely impaired respiration and lipoic acid metabolism and result in infantile-onset mitochondrial encephalopathy, non-ketotic hyperglycinemia, myopathy, lactic acidosis, and early death.[13-15] However, little is known about the physiological function of ISCA1 in vivo. To gain further insights into the function of mammalian ISCA1 in vivo, we generated a systematic *ISCA1* knockout rat by knocking in the *mCherry-Cre* cassette at the *ISCA1* locus. The rats were then used to examine the expression pattern of ISCA1 and analyze the embryo development.

2 | MATERIALS AND METHODS

2.1 | Animals

The Sprague-Dawley (SD) *Rosa26-imCherry* rats were generated in our lab as reported previously.[16] The floxed *eGFP* and *mCherry* cassette was inserted in the *Rosa26* locus and the expression of *mCherry* was induced in the presence of Cre protein, which was used as Cre reporter rat strain. The *ISCA1* knockout rats were generated by insertion of *mCherry-Cre* at the *ISCA1* locus as described previously.[17] Briefly, we constructed two sgRNA expression vectors ($sgRNA_1$: GGACTGTCCAATGATGAAGC, $sgRNA_2$: GGCAGTCGTGCCCAAGAGGG), which were prepared using MEGA shortscript T7 Transcription kit (Ambion). The plasmid containing two homologous arms and a cassette of *mCherry-p2a-Cre* fusion gene was constructed as a knock-in donor.

The fertilized eggs from female SD rat donors (Huafukang) were prepared following the protocols described previously.[17,18] The microinjection mixture, which contained Cas9 protein (30 ng/μL), the two sgRNAs (each 10 ng/μL) and donor DNA (4 ng/μL), was pre-warmed at 37°C for 20 minutes before microinjection. The microinjection mixture was microinjected into both the cytoplasm and the male pronucleus of the fertilized eggs with a Nikon Microinjection system following standard protocols. After microinjection, the zygotes were transferred to pseudopregnant SD rats (20-30 zygotes per pseudopregnant rat), which subsequently gave birth to live pups. The litters were then genotyped by PCR using the following primers: 5′-CATGGAGAGAAGCTGAGGTCC-3′, 5′- TCTCACGCTGTCTTGATTCTAAGC-3′ and 5′-GGTGTAGTCCTCGTTGTGGG-3′. The 423 bp fragments (wild type [WT]) were amplified with 30 PCR cycles consisting of 94°C for 30 seconds, 61°C for 30 seconds and 72°C for 30 seconds, and the 702 bp fragments (knockout) were amplified with 30 PCR cycles consisting of 94°C for 30 seconds, 60°C for 30 seconds and 72°C for 60 seconds.

All the rats used in this study were maintained on a SD background and bred in an AAALAC-accredited facility. The use of animals in the current study was approved by the Animal Care and Use Committee of the Institute of Laboratory AnimalScience of Peking Union Medical College (ZLF18003).

2.2 | Embryo collection

For rat embryo preparation, female and male heterozygous rats (1:1) were put in a special cage overnight, and those females with a vaginal plug on the following morning were regarded as 0.5 day pregnant at noon that day. The female and male rats were then separated. The embryos were sampled at 2.5 days and 8.5 days. The embryos were then used for morphologic observation or Western blot.

2.3 | Histological observation

The rats were sacrificed and fixed by perfusion of 4% paraformaldehyde solution. The tissues were sampled and frozen sections of the tissues were prepared using a standard procedure. The frozen sections were then examinated and the images were captured using the NanoZoomer family of Digital Pathology Systems (NDP) (NanoZoomer S60).

2.4 | Reverse transcription PCR

Total RNA was extracted from the tissues using a mirVana™ miRNA Isolation Kit (Ambion) and the cDNA was obtained by reverse transcription of RNA using a miScript II RT Kit (Qiagen). The cDNA of ISCA1 from different tissues was amplified by PCR using the primers 5′-CAAGAGAACACTGCAACCCAC-3′ and 5′-ACACCCACTTTCAGACCCAC-3′. The PCR was conducted for 26 cycles of 94°C for 30 seconds, 60°C for 30 seconds and 72°C for 30 seconds. The relative expression of ISCA1 was calculated using gray scanning and normalized to GADPH (Image J).

2.5 | Western blot

Male and female heterozygous rats were mated and the WT and homozygous embryos were identified and same-genotype embryos were combined for analysis. The combined embryo lysates of were separated on 12% SDS-PAGE. Western blot

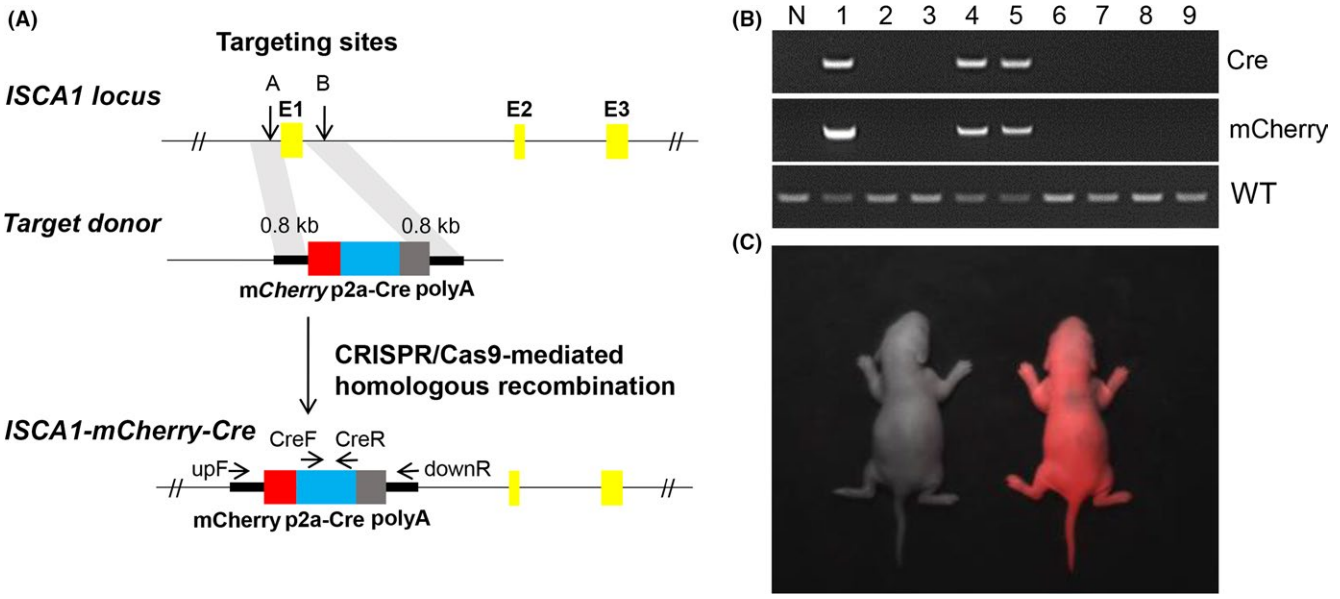

FIGURE 1 The establishment of *ISCA1* knockout rats. A, The *mCherry-Cre* cassette was knocked in at the *ISCA1* locus, replacing the exon1 of *ISCA1* gene. B, The mutated rats were genotyped by PCR. C, The heterozygous *ISCA1-mCherry-Cre* rats (*ISCA1 mCherry-Cre*$^{-/+}$) were crossed with the *Rosa26-imCherry* reporter rats. A strong expression of mCherry protein was induced by Cre (right) compared with a WT rat (left). The mCherry fluorescence images were captured by In-Vivo Imaging Systems

was performed according to standard procedures. The primary antibodies for NADH dehydrogenase [ubiquinone] 1 alpha subcomplex subunit 9 (NDUFA9, 1:1000, Abcam, ab14713), and aconitase 2 (ACO2, 1:1000, Abcam, ab110321) were visualized using anti-mouse HRP-conjugated secondary antibody (Santa Cruz Biotechnology, Inc.), and TOMM20 (1:250, Ivitrogen, PA5-52843) was visualized using anti-rabbit HRP-conjugated secondary antibody (Santa Cruz Biotechnology, Inc.). Quantitative analysis was performed by densitometry using NIH Image software and normalized to TOMM20.

2.6 | Statistical analysis

The statistical significance of differences between two groups was analyzed using the independent-samples *t* test. Data were presented as the means ± SD. The differences were considered to be significant at $P < 0.05$.

3 | RESULTS

3.1 | Generation of *ISCA1* knockout rats

The *mCherry* and *Cre* genes were fused via a *p2a* sequence to construct a *mCherry-Cre* cassette. The exon1 of the *ISCA1* gene was replaced by *mCherry-Cre* using CRISPR/Cas9 genomic editing (Figure 1A,B) and resulted in the deletion of the start codon in exon1 for *ISCA1*, causing *ISCA1* knockout. In total, 60 zygotes were transferred to two pseudopregnant SD rats and nine litters were delivered. Three litters with the *mCherry-Cre* fusion gene were detected and confirmed by DNA sequencing.

The rat line with *mCherry-Cre* knock-in at the *ISCA1* locus is referred to as *ISCA1-mCherry-Cre* (officially named SD.ISCA1(TM-mCherry-Cre)-GC/ILAS in our rat resource database [www.ratresource.com]).

The promoter of *ISCA1* drove the *mCherry-Cre* cassette to express mCherry and Cre proteins and allowed us to examine the ISCA1 expression pattern either directly via the *mCherry* reporter gene or, when crossed with *Rosa26-imCherry*, indirectly using Cre activity. Cre induced stronger expression of *mCherry* in *Rosa26-imCherry* rats and was appropriate for intravital imaging. The intravital imaging result showed that mCherry was generally observed and suggested that the ISCA1 was expressed broadly in whole body of the rats (Figure 1C). Furthermore, heterozygous rats (*ISCA1-mCherry-Cre*$^{-/+}$) showed no difference compared with WT rats in fertility, food uptake, body weight and lifespan (data not shown).

3.2 | Expression pattern of ISCA1 in tissues of rats

The tissues of heart, muscle, cerebrum, cerebellum, liver, spleen, lung, kidney, thymus, gut, ovary, and testis from *ISCA1-mCherry-Cre*$^{-/+}$ rats were sampled and the frozen sections of those tissues were observed under Digital Pathology Systems. The results showed that mCherry, directly driven by the ISCA1 promoter, was observed in all of these tissues. These results suggested that ISCA1 was expressed broadly (Figure 2A). The expression of *ISCA1* mRNA was selectively confirmed by RT-PCR in the tissues of heart, liver, spleen, lung, kidney, muscle, fat, and brain (Figure 2B) and quantified by gray scanning, normalized to GADPH (Figure 2C, n = 6). The results showed that *ISCA1* mRNA was expressed in all eight tissues and expression levels were higher in the spleen, heart, and brain compared with other tissues.

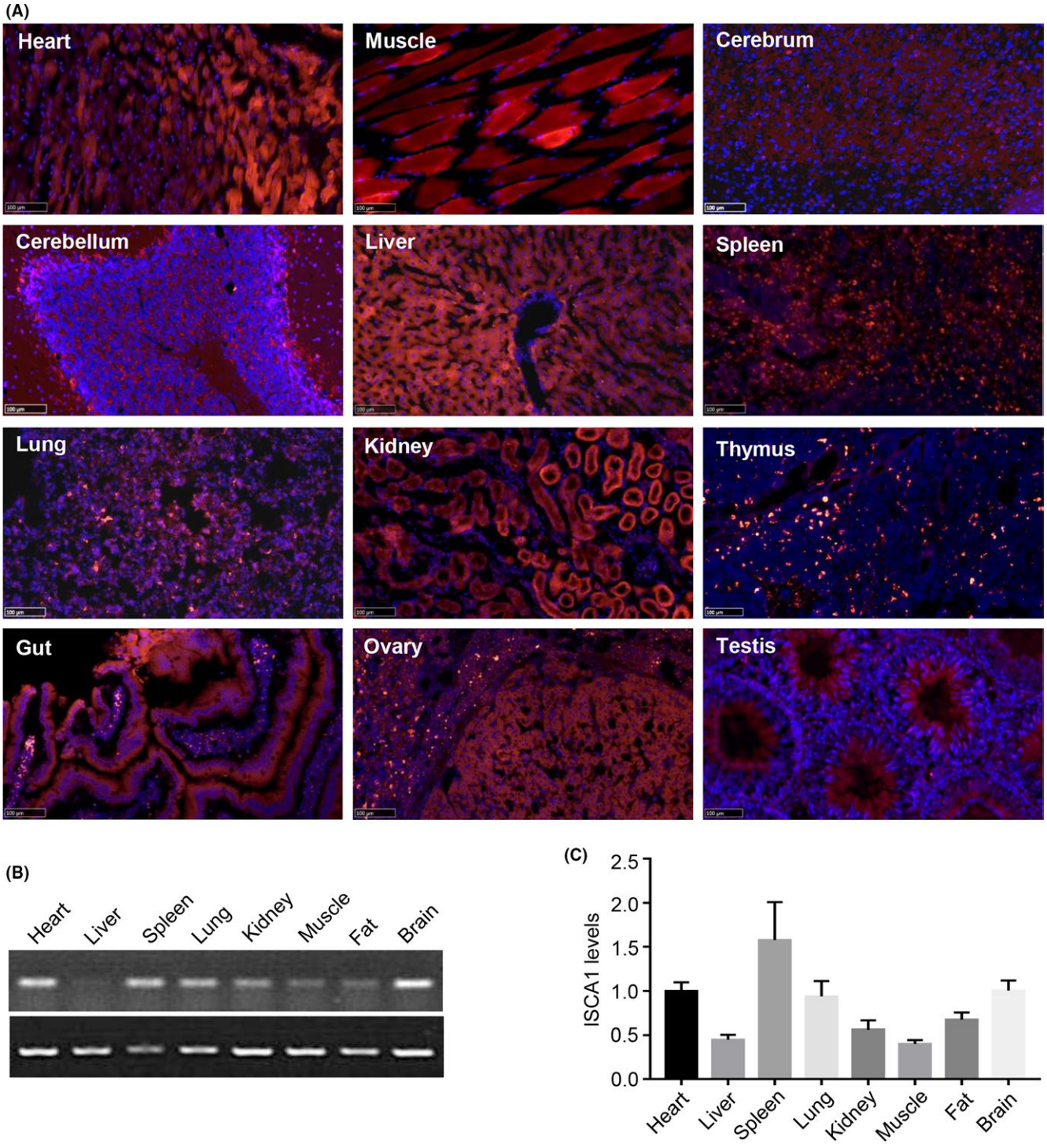

FIGURE 2 The expression pattern of ISCA1. A, The tissues of *ISCA1-Cre-mCherry* $^{-/+}$ rats were sampled and frozen sections of the tissues were examined using the NanoZoomer family of Digital Pathology Systems (magnification× 40, scale bar = 100 μm). B, The expression of ISCA1 in the tissues was further analyzed by RT-PCR and C, quantified by gray scanning and normalized to GADPH (n = 6)

3.3 | Embryonic lethality of homozygous *ISCA1-mCherry-Cre* rats

The exon1 of the *ISCA1* gene was replaced by *mCherry-Cre*, resulting in the knockout of *ISCA1*. The heterozygous rats were normal, but no homozygous rats (*ISCA1-mCherry-Cre*$^{-/-}$) were detected among the 83 litters produced by mating between heterozygous rats from the f1 to the f4 generation (Figure 3A). The result suggested that knockout of ISCA1 resulted in embryonic lethality. We then observed the embryonic morphology at 2.5 and 8.5 days. The *ISCA1-mCherry-Cre*$^{-/-}$ embryos were normally developed at the 4-cell stage (Figure 3B) and but abnormal

(A)

Gene types	Number
WT	27
Heterozygote	56
Homozygote	0
Total	83

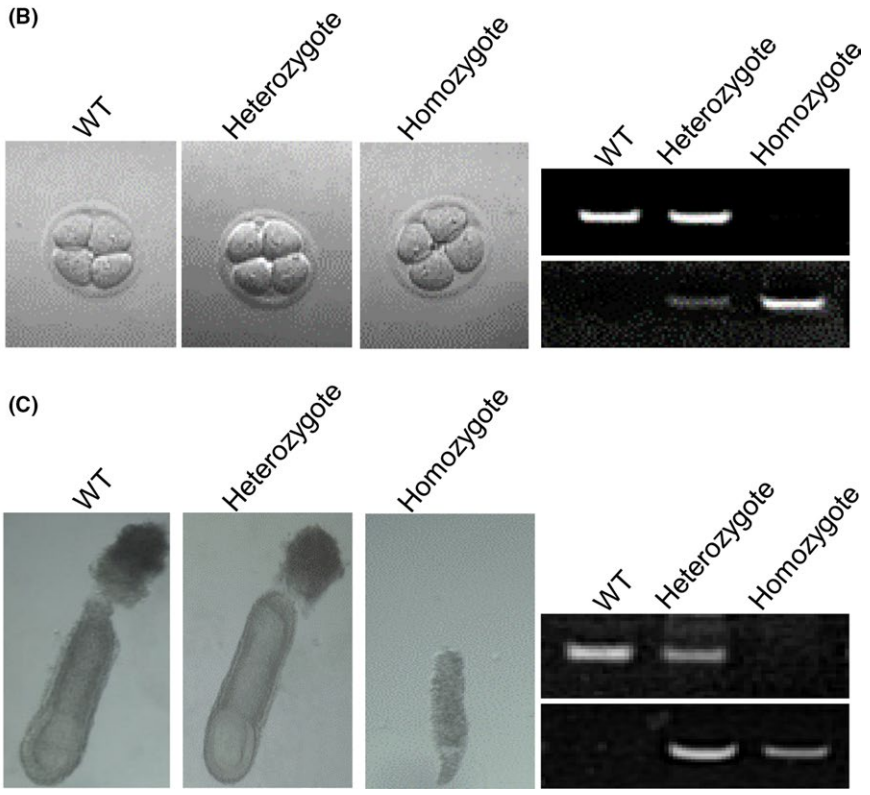

FIGURE 3 Observation of the *mCherry-Cre* $^{-/-}$ embryos. A, The male and female heterozygous rats (*ISCA1-mCherry-Cre*$^{-/+}$) were mated with each other and the numbers of WT, heterozygote and homozygote litters (*ISCA1-mCherry-Cre*$^{-/-}$) were counted. The embryonic morphology was observed and genotyped at B, 2.5 d, and C, 8.5 d

development or development block were observed in embryo at 8.5 days (Figure 3C).

3.4 | The expression of key proteins of the electron transport chain and TCA cycle

NDUFA9 protein is a key protein for electron transport chain, which is essential for stabilizing the junction between the membrane and matrix arms of complex I. The Western blot results showed that NDUFA9 protein was 40% lower in the *ISCA1-mCherry-Cre*$^{-/-}$ embryos compared with the WT embryos (Figure 4A,B). ACO2 protein is a tricarboxylic acid (TCA) cycle enzyme that converts citrate to isocitrate. The Western blot results showed that ACO2 protein was 60% higher in the *ISCA1-mCherry-Cre*$^{-/-}$ embryos compared with the WT embryos (Figure 4A,C). These results suggested that the ISCA1 knockout resulted in damage to the electron transport chain and TCA cycle.

4 | DISCUSSION

MMDS is characterized by impairment of mitochondria and affects infants. The typical clinical manifestations of MMDS include severe brain dysfunction, seizures, and psychomotor delay.[19] It is also associated with lung hypertension or cardiomyopathy.[20] MMDS is a genetic disease caused by mutations in the genes encoding components of the Fe/S biogenesis machinery including the NFU1 iron-sulfur cluster scaffold (*NFU1*), BolA family member 3 (*BOLA3*), iron-sulfur cluster assembly factor homolog IBA57 (*IBA57*) and *ISCA2*.[14,19-22] *ISCA1* is a recently discovered causal gene for MMDS identified in two unrelated

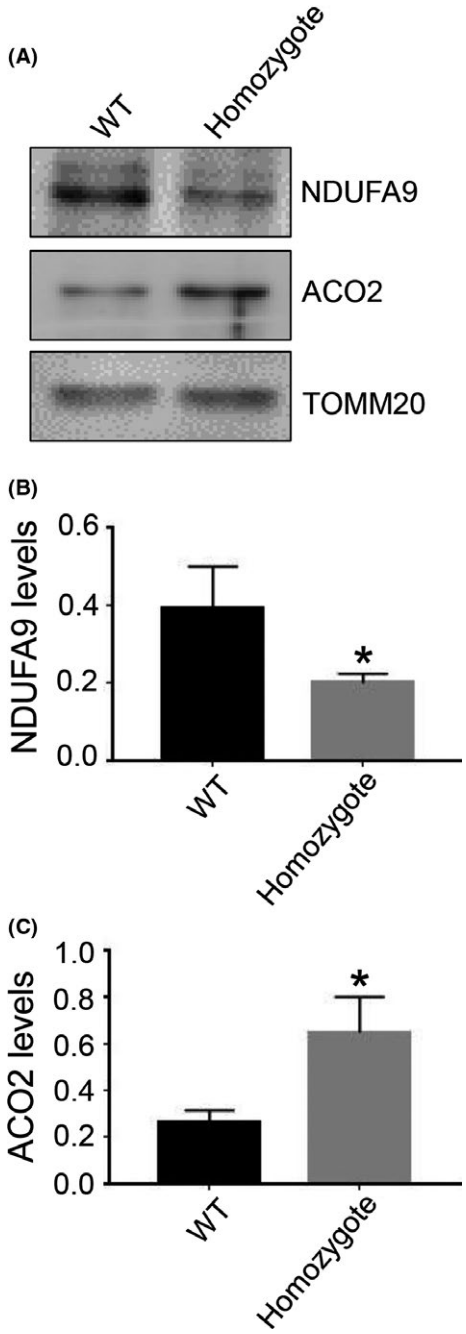

FIGURE 4 The expression of NDUFA9 and ACO2. A, The total embryo lysates from WT and homozygous embryos (*ISCA1-mCherry-Cre*$^{-/-}$) were separated on SDS-PAGE and the expression levels of NDUFA9 and ACO2 detected by Western blot. The levels of B, NDUFA9 protein and C, ACO2 protein were quantified by gray scanning and normalized to TOMM20 (n = 3, *$P < 0.05$)

Indian families[13], and is a key component of the Fe/S biogenesis process. We generated an ISCA1 knockout rat line by replacing exon1 of *ISCA1* with the *mCherry-Cre* fusion gene (Figure 1A,B). Interestingly, an attempt has been made to use ISCA1 as a magnetic protein, to induce magnetic activation of neuronal activity with a magnet receptor.[23] The ISCA1 expression pattern is therefore of particular interest in rats. We detected ISCA1 expression by intravital imaging, histological observation and RT-PCR. The results indicated that ISCA1 was expressed broadly throughout the body in the rats (Figures 1 and 2). We did not observe any specific expression of ISCA1 in the brain, which suggested that endogenous ISCA1 does not function as a magnetic protein to induce magnetic activation in neurons.

ISCA1 knockout resulted in developmental block in embryos at 8.5 days and caused embryonic lethality (Figure 3). The ISCA1 protein accepts Fe/S from a scaffold protein and transfers it to the respiratory complex.[12] The Fe/S is necessary for the stability of the mitochondrial Fe/S containing proteins of the respiratory complex in eukaryotic cells.[10,24] *ISCA1* knockdown by rAAV-mediated shRNA resulted in a substantial decrease in Succinate Dehydrogenase Complex Iron Sulfur Subunit B (SDHB), NADH Dehydrogenase Fe-S Protein 3 (NDUFS3) and NADH Dehydrogenase (Ubiquinone) Fe-S Protein 5 (NDUFS5) in skeletal muscle.[12] NDUFA9 is a Fe/S-containing protein of the mitochondrial respiratory chain complex I and is essential for assembling and stabilizing complex I.[25,26] It was found that the mutated *NDUFA9* gene caused a severe neonatally fatal phenotype in humans.[27] In *ISCA1* knockout rat embryos, the NDUFA9 protein decreased by 40% (Figure 4A,B).

The primary activity of ACO2 protein is to control cellular adenosine triphosphate (ATP) production via conversion of citrate to isocitrate.[28] Mutations or altered activity of ACO2 are associated with diseases such as epilepsy, brain atrophy, optic atrophy, retinal degeneration, and Huntington's Disease.[29-31] Our results showed that ACO2 protein increased by 60% in *ISCA1* knockout embryos (Figure 4A,C), unlike the observed decrease in Fe/S transfer protein. ACO2 is central to carbohydrate and energy metabolism and is associated with multiple metabolic pathways and pathologic conditions such as Huntington's Disease[31], hypoxia[32], and reactive oxygen species (ROS)[33] and energy metabolism defects.[34] ACO2 production could be regulated by cell energy metabolism and the observed increase in ACO2 activity might counteract cell energy metabolism defects.[34] We speculated that the *ISCA1* knockout resulted in damage to the mitochondrial respiratory chain complex I via a decrease in NDUFA9 protein, leading to defective energy metabolism. This, in turn, induced the increase in ACO2 levels seen in the rat embryos. The mechanism for the upregulation of ACO2 by *ISCA1* knockout requires further study.

In summary, *ISCA1* is a gene expressed throughout the body and its knockout caused early embryonic death in rats. The *ISCA1* knockout resulted in damage to the electron transport chain and energy metabolism.

ACKNOWLEDGEMENTS

The present work was supported in part by the CAMS Innovation Fund for Medical Sciences (CIFMS, 2017-I2M-3-015, 2016-I2M-1-004).

CONFLICT OF INTEREST

None.

AUTHOR CONTRIBUTIONS

All listed authors meet the requirements for authorship. LFZ and DL conceived the idea, designed the experiment and wrote the main manuscript. XLY and XZ performed the main experiments. XLY analyzed the data. YWM and DW completed the design and construction of the animal model. WC and SG completed microinjection and some animal experiments. All authors have read and approved the manuscript.

ORCID

Xinlan Yang https://orcid.org/0000-0002-3030-7658
Yuanwu Ma https://orcid.org/0000-0002-1882-1777

REFERENCES

1. Beilschmidt LK, Puccio HM. Mammalian Fe-S cluster biogenesis and its implication in disease. *Biochimie*. 2014;100:48-60.
2. Lill R. Function and biogenesis of iron-sulphur proteins. *Nature*. 2009;460(7257):831-838.
3. Huber C, Eisenreich W, Hecht S, Wachtershauser G. A possible primordial peptide cycle. *Science*. 2003;301(5635):938-940.
4. Zeng J, Geng M, Jiang H, Liu Y, Liu J, Qiu G. The IscA from Acidithiobacillus ferrooxidans is an iron-sulfur protein which assemble the [Fe4S4] cluster with intracellular iron and sulfur. *Arch Biochem Biophys*. 2007;463(2):237-244.
5. Colin F, Martelli A, Clemancey M, et al. Mammalian frataxin controls sulfur production and iron entry during de novo Fe4S4 cluster assembly. *J Am Chem Soc*. 2013;135(2):733-740.
6. Brazzolotto X, Gaillard J, Pantopoulos K, Hentze MW, Moulis JM. Human cytoplasmic aconitase (Iron regulatory protein 1) is converted into its [3Fe-4S] form by hydrogen peroxide in vitro but is not activated for iron-responsive element binding. *J Biol Chem*. 1999;274(31):21625-21630.
7. Brill AS. Transition metals in biochemistry. *Mol Biol Biochem Biophys*. 1977;26:III-VIII, 1-186.
8. Sheftel A, Stehling O, Lill R. Iron-sulfur proteins in health and disease. *Trends Endocrinol Metab*. 2010;21(5):302-314.
9. Sheftel AD, Stehling O, Pierik AJ, et al. Humans possess two mitochondrial ferredoxins, Fdx1 and Fdx2, with distinct roles in steroidogenesis, heme, and Fe/S cluster biosynthesis. *Proc Natl Acad Sci U S A*. 2010;107(26):11775-11780.
10. Sheftel AD, Wilbrecht C, Stehling O, et al. The human mitochondrial ISCA1, ISCA2, and IBA57 proteins are required for [4Fe-4S] protein maturation. *Mol Biol Cell*. 2012;23(7):1157-1166.
11. Tong WH, Rouault TA. Functions of mitochondrial ISCU and cytosolic ISCU in mammalian iron-sulfur cluster biogenesis and iron homeostasis. *Cell Metab*. 2006;3(3):199-210.
12. Beilschmidt LK, Ollagnier de Choudens S, Fournier M, et al. ISCA1 is essential for mitochondrial Fe4S4 biogenesis in vivo. *Nat Commun*. 2017;8:15124.
13. Shukla A, Hebbar M, Srivastava A, et al. Homozygous p.(Glu87Lys) variant in ISCA1 is associated with a multiple mitochondrial dysfunctions syndrome. *J Hum Genet*. 2017;62(7):723-727.
14. Al-Hassnan ZN, Al-Dosary M, Alfadhel M, et al. ISCA2 mutation causes infantile neurodegenerative mitochondrial disorder. *J Med Genet*. 2015;52(3):186-194.
15. El-Hattab AW, Scaglia F. Mitochondrial cytopathies. *Cell Calcium*. 2016;60(3):199-206.
16. Ma Y, Yu L, Pan S, et al. CRISPR/Cas9-mediated targeting of the Rosa26 locus produces Cre reporter rat strains for monitoring Cre-loxP-mediated lineage tracing. *FEBS J*. 2017;284(19):3262-3277.
17. Ma Y, Chen W, Zhang X, et al. Increasing the efficiency of CRISPR/Cas9-mediated precise genome editing in rats by inhibiting NHEJ and using Cas9 protein. *RNA Biol*. 2016;13(7):605-612.
18. Ma Y, Zhang X, Shen B, et al. Generating rats with conditional alleles using CRISPR/Cas9. *Cell Res*. 2014;24(1):122-125.
19. Ahting U, Mayr JA, Vanlander AV, et al. Clinical, biochemical, and genetic spectrum of seven patients with NFU1 deficiency. *Front Genet*. 2015;6:123.
20. Ajit Bolar N, Vanlander AV, Wilbrecht C, et al. Mutation of the iron-sulfur cluster assembly gene IBA57 causes severe myopathy and encephalopathy. *Hum Mol Genet*. 2013;22(13):2590-2602.
21. Navarro-Sastre A, Tort F, Stehling O, et al. A fatal mitochondrial disease is associated with defective NFU1 function in the maturation of a subset of mitochondrial Fe-S proteins. *Am J Hum Genet*. 2011;89(5):656-667.
22. Baker PR II, Friederich MW, Swanson MA, et al. Variant non ketotic hyperglycinemia is caused by mutations in LIAS, BOLA3 and the novel gene GLRX5. *Brain*. 2014;137(Pt 2):366-379.
23. Long X, Ye J, Zhao D, Zhang SJ. Magnetogenetics: remote non-invasive magnetic activation of neuronal activity with a magnetoreceptor. *Sci Bull (Beijing)*. 2015;60:2107-2119.
24. Guillon B, Bulteau AL, Wattenhofer-Donze M, et al. Frataxin deficiency causes upregulation of mitochondrial Lon and ClpP proteases and severe loss of mitochondrial Fe-S proteins. *FEBS J*. 2009;276(4):1036-1047.
25. Baertling F, Sanchez-Caballero L, van den Brand MAM, et al. NDUFA9 point mutations cause a variable mitochondrial complex I assembly defect. *Clin Genet*. 2018;93(1):111-118.
26. Stroud DA, Formosa LE, Wijeyeratne XW, Nguyen TN, Ryan MT. Gene knockout using transcription activator-like effector nucleases (TALENs) reveals that human NDUFA9 protein is essential for stabilizing the junction between membrane and matrix arms of complex I. *J Biol Chem*. 2013;288(3):1685-1690.
27. van den Bosch BJ, Gerards M, Sluiter W, et al. Defective NDUFA9 as a novel cause of neonatally fatal complex I disease. *J Med Genet*. 2012;49(1):10-15.
28. Jung SJ, Seo Y, Lee KC, Lee D, Roe JH. Essential function of Aco2, a fusion protein of aconitase and mitochondrial ribosomal protein bL21, in mitochondrial translation in fission yeast. *FEBS Lett*. 2015;589(7):822-828.
29. Marelli C, Hamel C, Quiles M, et al. ACO2 mutations: a novel phenotype associating severe optic atrophy and spastic paraplegia. *Neurol Genet*. 2018;4(2):e225.
30. Spiegel R, Pines O, Ta-Shma A, et al. Infantile cerebellar-retinal degeneration associated with a mutation in mitochondrial aconitase, ACO2. *Am J Hum Genet*. 2012;90(3):518-523.
31. Chen CM, Wu YR, Chang KH. Altered aconitase 2 activity in huntington's disease peripheral blood cells and mouse model striatum. *Int J Mol Sci*. 2017;18(11):2480. http://doi: 10.3390/ijms18112480.
32. Cheresh P, Kim SJ, Tulasiram S, Kamp DW. Oxidative stress and pulmonary fibrosis. *Biochim Biophys Acta*. 2013;1832(7):1028-1040.
33. Sadat R, Barca E, Masand R, et al. Functional cellular analyses reveal energy metabolism defect and mitochondrial DNA depletion in a case of mitochondrial aconitase deficiency. *Mol Genet Metab*. 2016;118(1):28-34.
34. Tang M, Liu BJ, Wang SQ, et al. The role of mitochondrial aconitate (ACO2) in human sperm motility. *Syst Biol Reprod Med*. 2014;60:251-256.

How to cite this article: Yang X, Lu D, Zhang X, et al. Knockout of ISCA1 causes early embryonic death in rats. *Animal Model Exp Med*. 2019;2:18–24. https://doi.org/10.1002/ame2.12059